

Synthesis of Bis{(2-dimethylphosphino)ethane-1-thiolato}bis(*tert*-butylthiolato)-molybdenum(IV) and Its Cluster-Forming Reactions with FeCl₂ and CuBr

Yasuhiro Arikawa, Hiroyuki Kawaguchi, Kazuo Kashiwabara, and Kazuyuki Tatsumi*

Research Center for Materials Science and Department of Chemistry, Graduate School of Science, Nagoya University, Furo-cho, Chikusa-ku, Nagoya 464-8602, Japan

Received April 23, 1999

Reaction of Mo(S^tBu)₄ with 2 equiv of HSCH₂CH₂PMe₂ (Hdmsp) produced Mo(dmsp)₂(S^tBu)₂ (**1**) in high yield. Treatment of **1** with FeCl₂ and CuBr led to the formation of heterometallic clusters, [Mo(O)(dmsp)₂]₂FeCl₂ (**2**) and [MoBr(dmsp)₂(μ₃-S)Cu₂(μ₂-S^tBu)₂] (**3**), respectively. The structures of **1–3** were determined by X-ray analyses. Complex **1** assumes a distorted octahedral geometry with a cis-disposition of two ^tBuS ligands. In the structure of **2**, an FeCl₂ unit bridges two square-pyramidal Mo(O)(dmsp)₂ fragments through interactions between Fe and dmsp sulfur atoms, where the MoS₂Fe quadrilateral is puckered. Formation of **3** involves C–S bond cleavage of one ^tBuS ligand of **1** and rearrangement of ligands between the Mo and Cu coordination sites, resulting in the structure consisting of two MoCu₂BrS(dmsp)₂ cluster units and two ^tBuS bridges.

Introduction

The design for construction of molybdenum-based heterometallic thiolato/sulfido clusters relies on preparation of appropriate mononuclear building blocks having sulfur-donor ligands. Tetrathiomolybdate, [Mo(S₄)²⁻], has been used most broadly for such cluster synthesis,¹ while the homoleptic thiolate complex, Mo(S^tBu)₄, is also useful as a potential precursor.² Recently half-sandwich trisulfido complexes of group 6 transition metals, [(C₅Me₅)M(S)₃]⁻ (M = Mo, W), have been synthesized in our laboratory,³ and they were found to serve as convenient entries into various heterometallic sulfido clusters.⁴ For example, the reactions of (PPh₄)[(C₅Me₅)W(S)₃] with copper and silver compounds generated W/Cu(Ag) clusters with structural diversity.^{4d,e} We also reported that the preformed thiolato complex of molybdenum, (C₅Me₅)Mo(S^tBu)₃, was readily converted to an Mo₂Fe₂S₄ cubane cluster upon reacting

it with FeCl₃.⁵ In these cluster-forming reactions, the C₅Me₅ auxiliary ligand facilitates isolation of the resulting cluster complexes, by promoting their solubility and by increasing stability of the cluster structures.

On the other hand, we explored coordination chemistry of late-transition metal complexes consisting of phosphorus–sulfur mixed-donor ligands Me₂PCH₂CH₂SR (R = H, CH₃), in which the phosphine moiety carries sterically undemanding and strongly electron-donating methyl groups.^{6a} We are now interested in expanding the scope of chemistry of molybdenum-based heterometallic clusters by utilizing the P–S hybrid ligand in an anionic form, Me₂PCH₂CH₂S⁻ (= dmsp⁻). The presence of a phosphino group in the proximity of a thiolate sulfur may modify the electronic property and coordination geometry of building units of cluster complexes.⁶ This paper describes the synthesis of Mo(S^tBu)₂(dmsp)₂ (**1**), and its cluster forming reactions with simple metal halides, FeCl₂ and CuBr, to give [Mo(O)(dmsp)₂]₂FeCl₂ (**2**) and [MoBr(dmsp)₂(μ₃-S)Cu₂(μ₂-S^tBu)₂] (**3**), respectively.

Results and Discussion

Synthesis of Mo(dmsp)₂(S^tBu)₂ (1**).** We first attempted to synthesize a homoleptic dmsp complex of molybdenum(IV) by the reaction of α-MoCl₄ with Lidmsp or Hdmsp/NEt₃. These reactions, however, did not give isolable products. On the other hand, when 2 equiv of Hdmsp was added to a reddish violet solution of Mo(S^tBu)₄ in THF, the solution immediately turned dark red. The ligand exchange reaction readily proceeded, and a crude product of Mo(dmsp)₂(S^tBu)₂ (**1**) was obtained as a dark-red crystalline solid in nearly quantitative yield upon removal of volatiles in vacuo. The complex **1** is very soluble in common organic solvents and was recrystallized from hexane with 76%

- (1) (a) Müller, A.; Diemann, E.; Jostes, R.; Bögge, H. *Angew. Chem., Int. Ed. Engl.* **1981**, *20*, 934–955. (b) Coucouvanis, D. *Acc. Chem. Res.* **1981**, *14*, 201–209. (c) Howard, K. E.; Rauchfuss, T. B.; Wilson, J. R. *Inorg. Chem.* **1988**, *27*, 3561–3567. (d) Manoli, J. M.; Potvin, C.; Secheresse, F.; Marzak, S. *Inorg. Chim. Acta* **1988**, *150*, 257–268. (e) Shibahara, T.; Akashi, H.; Kuroya, H. *J. Am. Chem. Soc.* **1988**, *110*, 3313–3314. (f) Holm, R. H. *Adv. Inorg. Chem.* **1992**, *38*, 1–71. (g) Evans, W. J.; Ansari, M. A.; Ziller, J. W.; Khan, S. I. *Organometallics* **1995**, *14*, 3–4. (h) Lang, J.; Tatsumi, K.; Kawaguchi, H.; Lu, J.; Ge, P.; Ji, W.; Shi, S. *Inorg. Chem.* **1996**, *35*, 7924–7927. (i) Ikada, T.; Kuwata, S.; Mizobe, Y.; Hidai, M. *Inorg. Chem.* **1998**, *37*, 5793–5797. (j) Hernandez-Molina, R.; Fedin, V. P.; Sokolov, M. N.; Sellsell, D. M.; Sykes, A. G. *Inorg. Chem.* **1998**, *37*, 4328–4334.
- (2) (a) Otsuka, S.; Kamata, M.; Hirotsu, K.; Higuchi, T. *J. Am. Chem. Soc.* **1981**, *103*, 3011–3014. (b) Payne, N. C.; Okura, N.; Otsuka, S. *J. Am. Chem. Soc.* **1983**, *105*, 245–251. (c) Lu, S.-W.; Okura, N.; Yoshida, T.; Otsuka, S.; Hirotsu, K.; Higuchi, T. *J. Am. Chem. Soc.* **1983**, *105*, 7470–7471.
- (3) (a) Kawaguchi, H.; Tatsumi, K. *J. Am. Chem. Soc.* **1995**, *117*, 3885–3886. (d) Kawaguchi, H.; Yamada, K.; Lang, J.; Tatsumi, K. *J. Am. Chem. Soc.* **1997**, *119*, 10346–10358.
- (4) (a) Lang, J.; Kawaguchi, H.; Ohnishi, S.; Tatsumi, K. *Chem. Commun.* **1997**, 405–406. (b) Lang, J.; Kawaguchi, H.; Tatsumi, K. *Inorg. Chem.* **1997**, *36*, 6447–6449. (c) Lang, J.; Tatsumi, K. *Inorg. Chem.* **1998**, *37*, 160–162. (d) Lang, J.; Kawaguchi, H.; Ohnishi, S.; Tatsumi, K. *Inorg. Chim. Acta* **1998**, *283*, 136–144. (e) Lang, J.; Kawaguchi, H.; Tatsumi, K. *J. Organomet. Chem.* **1998**, *569*, 109–119.

- (5) Kawaguchi, H.; Yamada, K.; Ohnishi, S.; Tatsumi, K. *J. Am. Chem. Soc.* **1997**, *119*, 10871–10872.
- (6) (a) Kita, M.; Yamamoto, T.; Kashiwabara, K.; Fujita, J. *Bull. Chem. Soc. Jpn.* **1992**, *65*, 2272–2274. (b) White, G. S.; Stephan, D. W. *Inorg. Chem.* **1985**, *24*, 1499–1503. (c) White, G. S.; Stephan, D. W. *Organometallics* **1987**, *6*, 2169–2175. (d) White, G. S.; Stephan, D. W. *Organometallics* **1988**, *7*, 903–910.

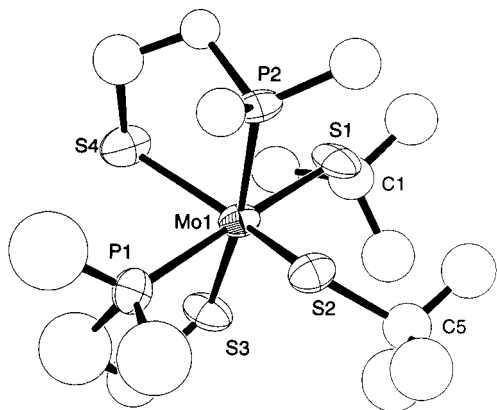


Figure 1. Molecular structure of $\text{Mo}(\text{dmosp})_2(\text{S}^t\text{Bu})_2$ (**1**). One of the two crystallographic independent molecules of **1** is drawn (molecule 1).

recovery. The ^1H NMR spectrum of **1** indicates paramagnetism of the $\text{Mo}(\text{IV})$ complex, and is not very informative. The molecular structure was established by the X-ray diffraction study, the formulation of which was consistent with the elemental analysis. The EI mass spectrum does not show signals of the parent molecular ion, but there appear a series of isotopic clusters associated with $[\text{Mo}(\text{S}^t\text{Bu})(\text{S})(\text{dmosp})_2]^+$, $[\text{MoS}_2(\text{dmosp})_2]^+$, and $[\text{MoS}(\text{dmosp})_2]^+$. The fragmentation of **1** occurs with a loss of *tert*-butyl and/or *tert*-butyl thiolate groups, indicating that the thiolates are labile and C–S bond cleavage occurs readily under the EI mass condition. Interestingly, however, the ^tBuS ligands remain intact upon addition of an excess Hdmosp to a THF solution of **1**. The selective formation of the phosphine-thiolato complex **1** is in sharp contrast to the reaction of $\text{Mo}(\text{S}^t\text{Bu})_4$ with PMe_2Ph , where the C–S bond rupture took place to yield $\text{Mo}_2(\mu\text{-S})_2(\text{S}^t\text{Bu})_4(\text{PMe}_2\text{Ph})_2$.⁷

The X-ray analysis shows that there are two independent molecules of **1** in an asymmetric unit. Their main structural features and metric parameters are nearly identical, except for the minor difference in orientation of the S^tBu groups as is incarnated by the torsional angles: $\text{P1-Mo1-S1-C1} = 11(8)^\circ$ (molecule 1) vs $\text{P3-Mo2-S5-C17} = -60(4)^\circ$ (molecule 2), $\text{S4-Mo1-S2-C5} = -176(1)^\circ$ vs $\text{S8-Mo2-S6-C21} = 170(1)^\circ$. The ORTEP drawing of molecule 1 is shown in Figure 1, and the selected bond distances and angles are compared with those of molecule 2 in Table 1. Either of the molecules assumes a distorted octahedral coordination geometry with a cis-disposition of two ^tBuS ligands. Given two dmosp and two ^tBuS ligands at Mo, there are five possible configurations, **A–E** as shown in Chart 1, without counting the enantiomers of **A–C**. Configurations **B** and **D** appear to be electronically less stable, because two phosphine P atoms, which are weaker donors relative to thiolate sulfurs, are trans to each other. On the other hand, methyl substituents of two phosphine groups come close to each other for configurations **C** and **E**, making the observed structure **A** most feasible by both electronic and steric reasons. However, the difference in stability between **A** and the other isomers would be small, and there remains a chance that the other configurations will also be isolated.

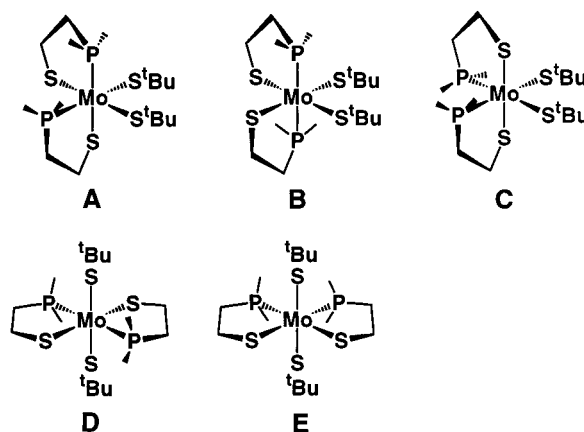
The Mo–S distances vary from 2.298(8) to 2.428(8) Å. The shortest bond occurs between Mo(1) and S(3) for molecule 1, and between Mo(2) and S(7) for molecule 2, which is understandable because either of the S atoms is situated trans to the Mo–P bond. The average of Mo–S distances (2.348 Å)

Table 1. Selected Bond Distances (Å) and Angles (deg) in **1**^a

molecule 1		molecule 2	
Bond Distances (Å)			
Mo1–S1	2.329(8)	Mo2–S5	2.338(8)
Mo1–S2	2.335(8)	Mo2–S6	2.349(8)
Mo1–S3	2.298(8)	Mo2–S7	2.311(8)
Mo1–S4	2.428(8)	Mo2–S8	2.399(9)
Mo1–P1	2.546(8)	Mo2–P3	2.528(9)
Mo1–P2	2.499(9)	Mo2–P4	2.506(9)
Bond Angles (deg)			
S1–Mo1–S2	101.9(3)	S5–Mo2–S6	100.4(3)
S3–Mo1–P1	82.0(3)	S7–Mo2–P3	80.8(3)
S4–Mo1–P2	79.3(3)	S8–Mo2–P4	77.4(3)
Mo1–S1–C1	123(1)	Mo2–S5–C17	122(1)
Mo1–S2–C5	116(1)	Mo2–S6–C21	116.7(10)

^a The numbering scheme for molecule 2 follows that assigned for molecule 1.

Chart 1



is longer than that of tetrahedral $\text{Mo}(\text{S}^t\text{Bu})_4$ (2.235(3) Å)^{2a} and is close to those of the octahedral $\text{Mo}(\text{IV})$ complexes, $\text{Mo}[\text{PhP}(\text{CH}_2\text{CH}_2\text{S})_2]_2$ (2.348 Å)⁸ and $\text{Mo}[\text{S}(\text{SCH}_2\text{CH}_2\text{S})_2]_2$ (2.361 Å).⁹ The mean Mo–P distance of 2.520 Å is somewhat longer than that of $\text{Mo}[\text{PhP}(\text{CH}_2\text{CH}_2\text{S})_2]_2$ (2.472 Å).⁸

Heterobimetallic Clusters Derived from $\text{Mo}(\text{dmosp})_2(\text{S}^t\text{Bu})_2$. It is known that thiolate ligands are capable of serving as potential bridging components for the construction of homo- and heterometallic clusters, because sulfur lone pairs of coordinated thiolate ligands may be bound to additional metal atoms.¹⁰ Here we describe intriguing cluster forming reactions of **1** with FeCl_2 and CuBr .

(a) Reaction with FeCl_2 . Treatment of **1** with FeCl_2 in THF at room-temperature resulted in the precipitation of a brown solid, which was recrystallized from CH_2Cl_2 /hexane to give $[\text{Mo}(\text{O})(\text{dmosp})_2]_2\text{FeCl}_2$ (**2**) as brown plates in 53% yield. A strong absorption band at 953 cm^{-1} in the IR spectrum of **2** indicates the presence of a terminal $\text{Mo}=\text{O}$ moiety, while the

(8) Blower, P. J.; Dilworth, J. R.; Leigh, G. J.; Neaves, B. D.; Normanton, F. B.; Hutchinson, J.; Zubieta, J. A. *J. Chem. Soc., Dalton Trans.* **1985**, 2647–2653.

(9) Hyde, J.; Magin, L.; Zubieta, J. *J. Chem. Soc., Chem. Commun.* **1980**, 204–205.

(10) (a) Osterloh, F.; Saak, W.; Haase, D.; Pohl, S. *Chem. Commun.* **1997**, 979–980. (b) Adams, H.; Bailey, N. A.; Gay, S. R.; Gill, L. J.; Hamilton, T.; Morris, M. J. *J. Chem. Soc., Dalton Trans.* **1996**, 2403–2407. (c) Kuwata, S.; Mizobe, Y.; Hidai, M. *J. Am. Chem. Soc.* **1993**, *115*, 8499–8500. (d) Li, P.; Curtis, M. D. *Inorg. Chem.* **1990**, *29*, 1242–1248. (e) Rousseau, R.; Stephan, D. W. *Organometallics* **1991**, *10*, 3399–3403. (f) Chojnacki, S. S.; Hsiao, Y.-M.; Darensbourg, M. Y.; Reibenspies, J. H. *Inorg. Chem.* **1993**, *32*, 3573–3576 and references therein.

(7) Kamata, M.; Yoshida, T.; Otsuka, S. *J. Am. Chem. Soc.* **1981**, *103*, 3572–3574.

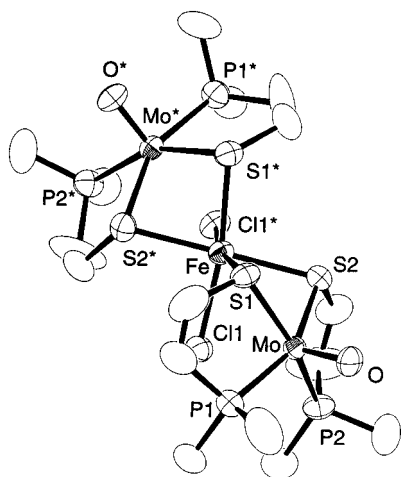


Figure 2. Molecular structure of [Mo(O)(dmsp)₂]₂FeCl₂ (**2**).

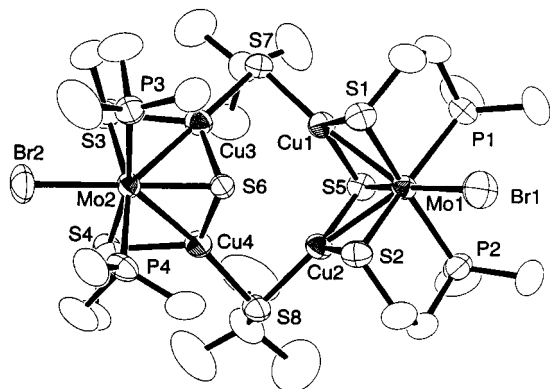


Figure 3. Molecular structure of [MoBr(dmsp)₂(μ₃-S)Cu₂]₂(μ₂-S^tBu)₂ (**3**).

Table 2. Selected Bond Distances (Å) and Angles (deg) in **2**

Bond Distances (Å)			
Mo—S1	2.423(2)	Mo—S2	2.426(2)
Mo—P1	2.469(2)	Mo—P2	2.468(2)
Mo—O	1.676(4)	Fe—Cl1	2.485(2)
Fe—S1	2.539(2)	Fe—S2	2.502(2)
Bond Angles (deg)			
S1—Mo—P1	82.27(7)	S2—Mo—P2	82.37(6)
S1—Mo—S2	82.32(6)	S1—Fe—S2	78.56(6)

¹H NMR spectrum exhibits broad resonances attributable to the dmsp ligands at δ 12.6, 3.90, and 1.94 ppm. Broadening of the ¹H NMR signals is presumably due to the paramagnetic nature of **2**. The EI mass spectrum does not show a signal arising from the parent molecule, but is characterized by an isotope cluster corresponding to [Mo(O)(dmsp)₂]⁺. Elemental analysis was in agreement with the proposed formulation of **2**, and the molecular structure was determined by the X-ray diffraction study. The oxo ligand in **2** is most probably derived from adventitious H₂O contained in hygroscopic FeCl₂, and we have not been successful in isolating an oxo-free 1:1 or 2:1 Mo/Fe cluster compound, even if FeCl₂ was predried overnight in vacuo at 110 °C and the reaction was carried out in a glovebox.

The X-ray derived molecular structure is shown in Figure 2, and the selected geometrical parameters are listed in Table 2. A crystallographic 2-fold axis runs through the Fe atom, bisecting the Cl—Fe—Cl' angle, and the two square-pyramidal Mo(O)(dmsp)₂ units are crystallographically equivalent. If the oxidation state of Fe is regarded as divalent, the Mo atoms are both tetravalent. The central Fe atom bridges these two molybdenum units through interactions with the dmsp sulfur

Table 3. Selected Bond Distances (Å) and Angles (deg) in **3**

Bond Distances (Å)			
Mo1—Cu1	2.6253(9)	Mo1—Cu2	2.628(1)
Mo2—Cu3	2.616(1)	Mo2—Cu4	2.619(1)
Mo1—Br1	2.657(1)	Mo2—Br2	2.6645(9)
Mo1—S1	2.410(2)	Mo1—S2	2.398(2)
Mo1—S5	2.282(2)	Mo2—S3	2.395(2)
Mo2—S4	2.411(2)	Mo2—S6	2.275(2)
Mo1—P1	2.505(2)	Mo1—P2	2.504(2)
Mo2—P3	2.510(2)	Mo2—P4	2.480(2)
Cu1—S1	2.239(2)	Cu1—S5	2.228(2)
Cu1—S7	2.196(2)	Cu2—S2	2.237(2)
Cu2—S5	2.228(2)	Cu2—S8	2.200(2)
Cu3—S3	2.241(2)	Cu3—S6	2.241(2)
Cu3—S7	2.213(2)	Cu4—S4	2.229(2)
Cu4—S6	2.235(2)	Cu4—S8	2.210(2)
Bond Angles (deg)			
S1—Mo1—S2	90.12(6)	S3—Mo2—S4	88.51(7)
P1—Mo1—P2	101.25(7)	P3—Mo2—P4	103.48(7)
S1—Mo1—S5	105.99(7)	S3—Mo2—S6	106.85(6)
S2—Mo1—S5	106.02(7)	S4—Mo2—S6	106.19(6)
S1—Cu1—S5	114.05(7)	S3—Cu3—S6	113.66(7)
S1—Cu1—S7	118.69(7)	S3—Cu3—S7	123.02(8)
S2—Cu2—S5	113.69(7)	S4—Cu4—S6	114.21(7)
S2—Cu2—S8	113.85(8)	S4—Cu4—S8	123.18(7)
Cu1—S7—Cu3	85.69(6)	Cu2—S8—Cu4	83.20(6)

atoms. The Fe atom forms octahedral coordination geometry with four dmsp sulfur atoms and two cis-disposed chlorine atoms. The MoS₂Fe quadrilateral is puckered. The dihedral angle between the MoS₂ and FeS₂ planes is 121°, and the degree of puckering is substantially higher than that observed for the related complex, (C₅H₅)₂Mo(μ₂-SⁿBu)₂FeCl₂ (dihedral angle = 148°).¹¹ Whereas the puckering deformation shortens the separation between Mo and Fe atoms, the observed Mo—Fe distance of 3.2873(6) Å is too long to invoke a metal—metal bonding. Thus the large puckering is not caused by an Mo—Fe interaction, and we reason the deformation in terms of an attractive interaction between Mo and Cl atoms. In the structure of **2**, each chloride ligand at Fe is placed in the close proximity to Mo (2.841(2) Å) at a position trans to the Mo=O bond. Due to the chelation of the thiolate sulfurs to Fe, the S1—Mo—S2 angle is narrowed (82.32(6)°), and the Mo—S bonds are elongated (av 2.425 Å), compared with the structure of **1**. Conversely, the P1—Mo—P2 angle is enlarged (103.28(7)°), and the Mo—P distances is shortened (av 2.469 Å). Interestingly, the Mo=O distance of 1.676(4) Å is notably shorter than that of the closely related complex Mo(O)(SCH₂CH₂PPh₂)₂ (1.733–(9) Å),¹² although it is not unusual for oxo-molybdenum (IV) complexes.¹³

(b) **Reaction with CuBr.** Complex **1** was allowed to react with 2 equiv of CuBr in THF at room temperature for 12 h, to find that color of the solution turned from dark red to dark brown. After removing an insoluble solid by centrifugation, hexane was added to the supernatant, from which dark red crystals of [MoBr(dmsp)₂(μ₃-S)Cu₂]₂(μ₂-S^tBu)₂ (**3**) were obtained in 53% yield. When 1 equiv of CuBr was reacted with **1**, only **3** was obtained in a lower yield (17%), and no other compounds could be isolated. The ¹H and ³¹P NMR spectra did not show assignable signals due to the paramagnetism of the complex, while the UV—visible spectrum in THF was featured by characteristic absorption at 270: 383 nm.

(11) Cameron, T. S.; Prout, C. K. *J. Chem. Soc., Chem. Commun.* **1971**, 161–162.

(12) Chatt, J.; Dilworth, J. R.; Schmutz, J. A.; Zubieta, J. A. *J. Chem. Soc., Dalton Trans.* **1979**, 1595–1599.

(13) Nugent, W. A.; Mayer, J. M. *Metal—Ligand Multiple Bonds*; John Wiley and Sons: New York, 1988.

Table 4. Crystal Data for Mo(dmsp)₂(S'Bu)₂ (**1**), [Mo(O)(dmsp)₂]₂FeCl₂ (**2**), and [MoBr(dmsp)₂(μ₃-S)Cu₂]₂(μ₂-S'Bu)₂ (**3**)

	1	2	3
formula	C ₁₆ H ₃₈ S ₄ P ₂ Mo	C ₁₆ H ₄₀ O ₂ S ₄ P ₄ Cl ₂ Mo ₂ Fe·2CH ₂ Cl ₂	C ₂₄ H ₅₈ Br ₂ S ₈ P ₄ Cu ₄ Mo ₂ ·C ₄ H ₈ O·1/2(C ₆ H ₁₄)
mol wt (g mol ⁻¹)	516.60	1005.12	1448.16
cryst syst	monoclinic	monoclinic	monoclinic
space group	C2/c (No. 15)	C2/c (No. 15)	P2 ₁ /c (No. 14)
color of crystal	dark red	brown	dark red
a (Å)	64.12(3)	14.740(2)	16.156(8)
b (Å)	9.195(4)	13.778(2)	13.482(3)
c (Å)	17.28(2)	19.537(2)	26.102(9)
β (deg)	93.63(5)	97.713(10)	100.92(3)
V (Å ³)	10169(11)	3931.7(7)	5582(3)
Z	16	4	4
ρ _{calc} (g cm ⁻³)	1.350	1.698	1.723
2θ _{max} (deg)	39.9	55	55
no. of unique rflns	2354	4700	13377
no. of obsd rflns	1508 ^a	2502 ^b	7404 ^b
no. of parameters	255	169	430
R ^c	0.073	0.041	0.043
Rw ^d	0.074	0.054	0.059
GOF ^e	1.38	1.11	1.07

^a Observation criterion $I > 1\sigma(I)$. ^b Observation criterion $I > 3\sigma(I)$. ^c $R = \sum||F_o| - |F_c||/\sum|F_o|$. ^d $R_w = \{\sum w(|F_o| - |F_c|)^2/\sum wF_o^2\}^{1/2}$. ^e $GOF = [\sum w(|F_o| - |F_c|)^2/(N_o - N_p)]^{1/2}$, where N_o and N_p denote the number of data and parameters, respectively.

The formulation of **3** was confirmed by the X-ray diffraction study, and the molecular structure is shown in Figure 3. The selected bond distances and angles are given in Table 3. The molecule **3** consists of two MoCu₂(Br)(S)(dmsp)₂ units linked by two 'BuS ligands which are bound to the Cu atoms. Formation of **3** from two molecules of **1** and four molecules of CuBr may be described by the following steps; (1) C–S bond cleavage of one 'BuS ligand of **1** generating μ₃-S; (2) migration of the other 'BuS ligand to a position bridging Cu atoms; and (3) migration of Br from the Cu coordination site to the Mo site. A consequence is liberation of two Br atoms and two 'Bu groups, although their fate is not clear at moment. During this reaction, the dmsp ligands at Mo remain intact. In the cluster core structure of **3**, four Cu atoms are nearly coplanar with the maximum deviation from the least-squares plane is 0.04 Å, and each of the μ₃-S atoms sits above (1.58 Å) or below (1.23 Å) the Cu₄ plane. On the other hand, the Mo atoms are both situated above the plane (0.88 and 1.19 Å), thus forming a boat conformation of Mo₂Cu₄. Provided that each Cu atom retains the original univalent oxidation state, the Mo atoms are again tetravalent. Each Mo atom assumes a distorted octahedral geometry, with the bromine and sulfido ligands being trans to each other, while the coordination geometry of each Cu is approximately trigonal-planar surrounded by three sulfurs. The Mo–Cu distances of 2.616(1)–2.628(1) Å indicate metal–metal bonding interactions.¹⁴ Interestingly, the bond lengths between the Cu atoms and the bridging 'BuS groups are notably shorter than the other Cu–S lengths. The average Mo–S(dmsp) distance of 2.404 Å is shorter by 0.021 Å than that of **2**, while the average Mo–P distance of 2.500 Å is longer by 0.031 Å. The Mo–μ₃-S bonds are obviously shorter than the Mo–S(dmsp) bonds, and their mean value of 2.279 Å is similar to that of (PPh₄)[(C₅Me₅)MoS₃Cu₃Br₃]₂ (2.291(2) Å).^{4d}

It is of interest to note that the reaction of Mo(S'Bu)₄ or *cis*-Mo(S'Bu)₂('BuNC)₂ with CuBr('BuNC)₃ was reported to give a binuclear complex ('BuNC)₄Mo(μ-S'Bu)₂CuBr,^{2b} and that a dinuclear complex [(C₅H₅)₂Ti(SCH₂CH₂PPh₂)₂Cu](BF₄) was synthesized by the reaction between (C₅H₅)₂Ti(SCH₂CH₂PPh₂)₂ and [Cu(CH₃CN)₄](BF₄).^{6b} In either case, the parent molecule,

to which CuBr or Cu is coordinated, retains its original structure. In contrast, C–S bond cleavage and ligand-shuffling took place in the cluster forming reaction of **1** with CuBr.

Experimental Section

General Procedure. All reactions were carried out using a standard Schlenk technique under an argon atmosphere. Solvents were dried and distilled before use according to the known methods. Hdmsp and Mo(S'Bu)₄ were prepared as reported.^{2a,6a} ¹H NMR spectra were recorded on a Varian UNITYplus-500 spectrometers, and chemical shifts are reported in ppm by reference to CDCl₃. For UV–visible spectra, a JASCO V-560 spectrometer was used. Infrared spectra were recorded on a Parkin-Elmer 2000FT-IR spectrometer. Mass spectra were collected on a Shimadzu QP5000 mass spectrometer. Elemental analyses were performed on a LECO-CHNS microanalyzer where the crystalline samples were sealed in thin silver tubes.

Preparation of Mo(dmsp)₂(S'Bu)₂ (1**).** To a THF (50 mL) solution of Mo(S'Bu)₄ (0.91 g, 2.01 mmol) was added 2 equiv of Hdmsp (0.62 g, 5.07 mmol). The color of the solution immediately changed from reddish violet to dark red. After the mixture was stirred for 2 h at room temperature, volatiles were removed in vacuo. The residue was extracted with hexane (75 mL), and concentration and cooling to 0 °C gave Mo(S'Bu)₂(dmsp)₂ (**1**) as dark red plates (0.79 g, 76%). IR (Nujol mull/KBr): 1412 w, 1359 s, 1288 m, 1158 m, 950 s cm⁻¹. UV–visible (λ_{max}; hexane): 264, 346, 486 nm. MS (EI): *m/z* 461 (M⁺ – C₄H₉), 404 (M⁺ – 2C₄H₉), 372 (M⁺ – C₄H₉ – SC₄H₉). Anal. Calcd for C₁₆H₃₈MoS₄P₂: C, 37.20; H, 7.41; S, 24.83. Found: C, 36.67; H, 7.48; S, 24.13.

Preparation of [Mo(O)(dmsp)₂]₂FeCl₂ (2**).** A THF (15 mL) solution of **1** (0.21 g, 0.41 mmol) was added to a slurry of FeCl₂ (60 mg, 0.47 mmol) in THF (15 mL). The color of the solution immediately became reddish brown. The reaction mixture was stirred at room temperature overnight, during which time a brown solid was formed. The solution was evaporated to dryness, and the residue was treated with CH₂Cl₂ to remove a yellow insoluble material by centrifugation. The CH₂Cl₂ solution was layered with hexane to afford [Mo(O)(dmsp)₂]₂FeCl₂ (**2**) as brown plates (90 mg, 53%). ¹H NMR (CDCl₃): δ 12.6 (s, 24H, PMe₂, Δν_{1/2} = 311 Hz), 3.90 (s, 8H, SCH₂, 25.0 Hz), 1.94 (s, 8H, PCH₂, 19.9 Hz). IR (Nujol mull/KBr): 1419 w, 1282 m, 932 m, 914 m, 953 (ν_{Mo=O}) s cm⁻¹. MS (EI): *m/z* 356 ([Mo(O)(dmsp)₂]⁺), 300 ([Mo(O)(dmsp)₂]⁺ – 2 C₂H₄). Anal. Calcd for C₁₈H₄₄O₂Cl₂P₄S₄FeMo₂: C, 21.51; H, 4.41; S, 12.76. Found: C, 21.86; H, 4.54; S, 12.82.

Preparation of [MoBr(dmsp)₂(μ₃-S)Cu₂]₂(μ₂-S'Bu)₂ (3**).** A THF (15 mL) solution of **1** (0.12 g, 0.23 mmol) was treated with CuBr (80 mg, 0.55 mmol) in THF (15 mL) at room temperature. The color of

(14) Gheller, S. F.; Hambley, T. W.; Rodgers, J. R.; Brownlee, R. T. C.; O'Connor, M. J.; Snow, M. R.; Wedd, A. G. *Inorg. Chem.* **1984**, *23*, 2519–2528 and references therein.

the solution gradually turned dark brown. After 12 h of stirring, the mixture was centrifuged to remove a yellow solid. The THF solution was layered with hexane to separate **3** as dark red crystals (80 mg, 53%). IR (Nujol mull/KBr): 1417 w, 1359 m, 1281 s, 952 s, 930 s, 912 m cm⁻¹. UV–visible (λ_{max} ; THF): 270, 383 nm. Anal. Calcd for C₂₄H₅₈Br₂P₄S₈Cu₄Mo₂: C, 21.62; H, 4.39. Found: C, 21.55; H, 4.80.

Crystal Structure Determinations of 1, 2, and 3. A dark-red crystal of **1** with dimensions 0.2 × 0.1 × 0.1 mm, a brown crystal of **2** with dimensions 0.4 × 0.25 × 0.1 mm, and a dark-red crystal of **3** with dimensions 0.5 × 0.5 × 0.3 mm were mounted in glass capillaries and sealed under argon. Diffraction data were collected at room temperature on a Rigaku AFC7R diffractometer employing graphite-monochromated Mo K α radiation ($\lambda = 0.71069 \text{ \AA}$) and using the ω -2 θ scan technique. The cell dimensions and their standard deviations were obtained from least squares refinements of 25 randomly selected centered reflections. Three standard reflections were monitored periodically for crystal decomposition or movement. The crystals of **2** and **3** showed only slight intensity variation (~1%) over the course of the data collections, while 12.8% decay was observed for **1**. The raw intensity data were corrected for Lorentz and polarization effects, and empirical absorption corrections based on ψ scans were applied.

All calculations were performed with the TEXSAN package. The structures of **1**, **2**, and **3** were solved by direct methods, which located

the metal-atom positions unequivocally. The other atoms were found in subsequent Fourier maps, and the structures were refined by full-matrix least squares. For **1**, the molybdenum, sulfur, and phosphorus atoms were anisotropically refined, and all carbon atoms were isotropically refined. In the case of **2**, each asymmetric unit contains a half molecule of **2** and one CH₂Cl₂ solvent molecule, and anisotropic refinements were applied to all non-hydrogen atoms. On the other hand, the crystal of **3** carries one entire molecule in each asymmetric unit along with one THF and a half hexane. All non-hydrogen atoms except for those of the solvent molecules were refined anisotropically. For all the structures, the hydrogen atoms were put at calculated positions with C–H distances of 0.97 Å. In the crystal structures of **2**, and **3**, no short contacts between the complex molecules and crystal solvents were observed. Important crystallographic data and the final R indices are summarized in Table 4, and complete crystallographic details are given in Supporting Information.

Supporting Information Available: Listings of X-ray crystallographic files, in CIF format, for **1**, **2**, and **3** are available free of charge on the Internet at <http://pubs.acs.org>.

IC990435R